Organic & Biomolecular Chemistry

ROYAL SOCIETY OF CHEMISTRY

PAPER

View Article Online
View Journal

Cite this: DOI: 10.1039/d0ob02095h

Structural isomers of saligenin-based β2-agonists: synthesis and insight into the reaction mechanism†

Anamarija Knežević, *[a,b] Jurica Novak,[c,d] Anita Bosak[e] and Marijana Vinković[f]

Salmeterol and albuterol are well-known β2-adenoreceptor agonists widely used in the treatment of inflammatory respiratory diseases, such as bronchial asthma and chronic obstructive pulmonary disease. Here we report the preparation of structural isomers of salmeterol and albuterol, which can be obtained from the same starting material as the corresponding β2-agonists, depending on the synthetic approach employed. Using 1D and various 2D NMR measurements, we determined that the structure of prepared isomers holds the β-aryl-β-aminoethanol moiety, in contrast to the α-aryl-β-aminoethanol moiety found in salmeterol and albuterol. We investigated the reaction of β-halohydrin and amines responsible for the formation of β-aryl-β-amino alcohol – both experimentally and using computational methods. The structure of β-halohydrin with the methyl salicylate moiety imposes the course of the reaction. The solvent plays a relevant, yet ambiguous role in the direction of the reaction, while the strength of the base influences the reaction yield and isomer ratio in a more evident way. Using computational methods, we have shown that the most probable reaction intermediate responsible for the formation of the unexpected isomer is the corresponding *para*-quinone methide, which can be formed due to phenol present in the methyl salicylate moiety. After successful preparation of albuterol and salmeterol isomers, we tested their inhibition potency to human acetylcholinesterase (AChE) and usual and atypical butyrylcholinesterase (BChE). Kinetic studies revealed that both isomers are low-potency reversible inhibitors of human cholinesterases.

Received 15th October 2020,
Accepted 16th November 2020

DOI: 10.1039/d0ob02095h

rsc.li/obc

1. Introduction

The vicinal amino alcohol moiety is a commonly found motif in naturally occurring molecules, from hydroxy amino acids to lipids and sugars.[1,2] Furthermore, it appears frequently in the structures of many synthetic molecules, from biologically active molecules to various catalysts.[3] In fact, the β-amino alcohol fragment is the key element in numerous pharmacologically important molecules such as antibiotics, β-blockers, β-adrenergic agonists, *etc*. The latter, potent bronchodilators widely used in the treatment of bronchial asthma, are in structural correlation with norepinephrine, a physiological neurotransmitter with a substituted β-phenylethylamine structure.[4,5] Therefore, a vast number of β2-agonist drugs possess the α-aryl-β-amino alcohol fragment in their structure (Fig. 1).

Given the importance of β-amino alcohol moiety in organic synthesis, numerous synthetic routes have been developed in order to control the regioselectivity and stereoselectivity of the final product.[1,2,6] Among functional group manipulation methods, the formation of amino alcohols *via* the reaction of an epoxide and an amine is commonly employed due to the availability of starting materials.[7] However, the regioselectivity

[a]*Division of Organic Chemistry and Biochemistry, Ruđer Bošković Institute, Bijenička cesta 54, 10000 Zagreb, Croatia. E-mail: Anamarija.Knezevic@irb.hr*
[b]*Faculty of Science and Technology, University of Twente, Drienerlolaan 5, 7522 NB Enschede, The Netherlands*
[c]*Laboratory of Computational Modeling of Drugs, Higher Medical and Biological School, South Ural State University, 20-A, Tchaikovsky Str., Chelyabinsk 454080, Russia*
[d]*Division of Physical Chemistry, Ruđer Bošković Institute, Bijenička cesta 54, Zagreb 10000, Croatia*
[e]*Biochemistry and Organic Analytical Chemistry Unit, Institute for Medical Research and Occupational Health, Ksaverska cesta 2, 10000 Zagreb, Croatia*
[f]*NMR Center, Ruđer Bošković Institute, Bijenička cesta 54, 10000 Zagreb, Croatia*

†Electronic supplementary information (ESI) available: File 1: ^{1}H and ^{13}C NMR spectra of products, detailed NMR information obtained from 2D NMR spectra and NOESY spectra of compounds **6** and **10**, Cartesian coordinates and computed total energies of complexes, IRC curves of transitions states. File 2: The normal mode of the transition state of the *para*-quinone methide – methylamine reaction complex leading to β-aryl-β-amino alcohol isomer with imaginary frequency of 139.4i cm^{-1}. File 3: The normal mode of the transition state of the bromo alcohol **3** – methylamine reaction complex leading to product **B** with imaginary frequency of 390.2i cm^{-1}. File 4: The normal mode of the transition state of the bromo alcohol **3** – methylamine reaction complex leading to product **A** with imaginary frequency of 413.2i cm^{-1}. See DOI: 10.1039/d0ob02095h

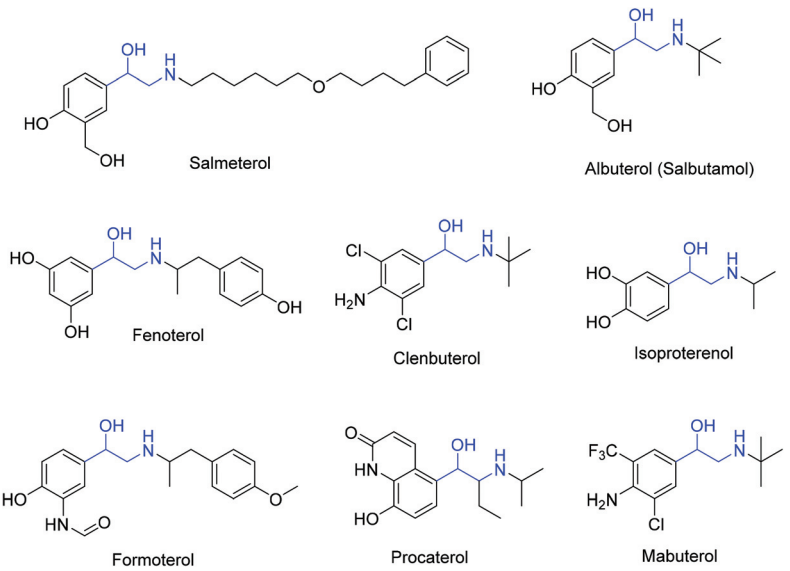

Fig. 1 Structures of bronchodilating β2-agonists.

depends substantially on the structures of the epoxide and the amine, as well as on reaction conditions (solvent, presence of acid, base or other catalyst such as metal salts).[8] Nevertheless, it has been widely used in the synthesis of numerous β-adrenergic agonists,[9–15] usually without discussing the regioselectivity of the ring opening.

Although the reaction of a β-halohydrin and an amine is less common, this synthetic approach has also been used for the preparation of several structurally analogous compounds, both using halohyrin with protected,[16–19] and unprotected hydroxyl group.[20–23] In the mentioned papers, β-halohydrin substitution was considered clear and simple, with α-aryl-β-amino alcohol being the only reported product. However, it seems that this reaction is not straightforward as expected. There have been reports on the β-aryl-β-amino alcohol being formed in the reaction instead of the desired product.[24] In fact, the synthesis of brombuterol was published using this approach,[25] and subsequently the structure of prepared compound was corrected to its β-aryl-β-amino alcohol isomer.[26] This nonclassical β-aryl-β-amino alcohol scaffold has been given the special attention in recent years due to the promising new bronchodilator isomer of mabuterol – trantinterol, the β2-adrenoceptor agonist currently being evaluated in clinical trials.[5,27] Based on the success of trantinterol, new potential bronchodilators with nonclassic β-aryl-β-amino alcohol scaffold have been developed, some of which have proven to be effective β2-adrenergic agonists (Fig. 2).[28,29]

We previously reported a study on the influence of some β2-agonists on the activity of human acetylcholinesterase (AChE; EC 3.1.1.7) and butyrylcholinesterase (BChE; E.C. 3.1.1.8).[30] We demonstrated that some β2-agonists, derivatives of resorcinol, catechol or saligenin, reversibly inhibited human acetylcholinesterase and butyrylcholinesterase and thus reduced their activity, affecting their roles in the organism. The saligenin

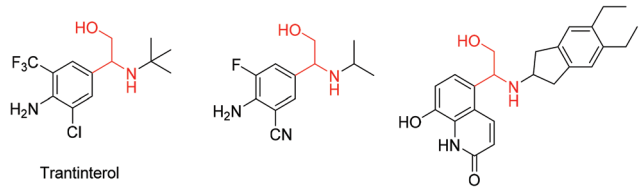

Fig. 2 Structure of trantinterol and new β2-agonists with β-aryl-β-amino alcohol scaffold.

derivative salmeterol, a well-known long-acting β2-adenoreceptor agonist used as an inhaled bronchodilator for the prevention of bronchospasm (Fig. 1),[31] was pointed out as the β2-agonist with the highest inhibition potency for both cholinesterases.[30] Here, we demonstrate that both salmeterol (**1**) and its β-aryl-β-amino alcohol isomer can be successfully obtained from the same starting material, depending on the synthetic approach used. Furthermore, the preparation of α-aryl-β-aminoethanol moiety is not always straightforward, and structural isomer can be obtained in the reaction of amine and β-halohydrin.

2. Results and discussion

Retrosynthetic analysis for the preparation of salmeterol starting from commercially available methyl 5-acetylsalicylate is shown in Scheme 1.

In the first synthetic route, methyl 5-acetylsalicylate was brominated at the α-position yielding **2**,[32] which was reduced to methyl 5-(2-bromo-1-hydroxy-ethyl)-salicylate (**3**) in the next step (Scheme 2). The reaction of **3** and amine **4** in acetonitrile with the help of triethylamine as the base produced product **6**. After reduction, white solid **7** was obtained, with the same molecular peak in MS, and the same number of signals in ^{1}H

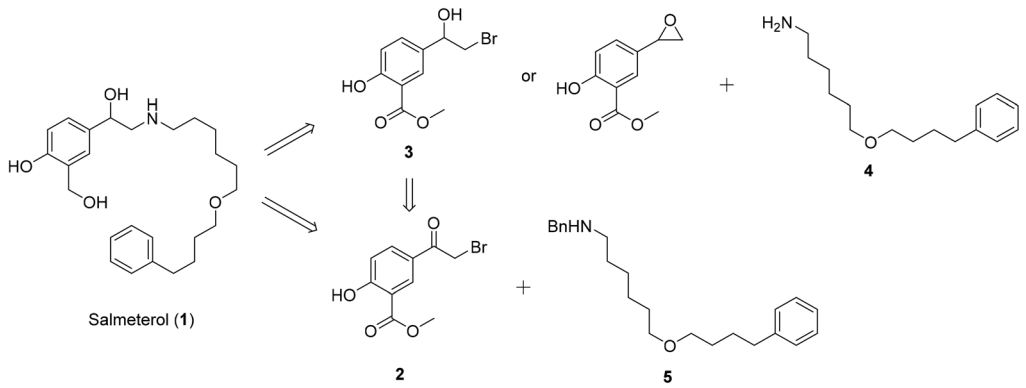

Scheme 1 Strategy for the preparation of salmeterol.

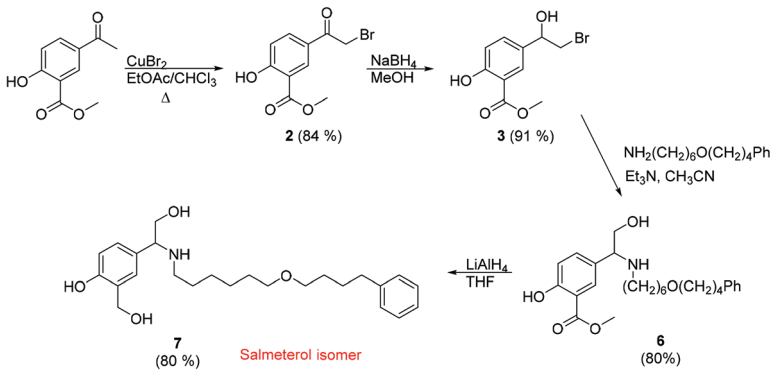

Scheme 2 Preparation of compound **7**.

and ^{13}C NMR spectra as salmeterol. However, a few of the signals in the NMR spectra were shifted when compared with the literature data for salmeterol (ESI†). Therefore, in order to resolve this discrepancy, the second synthetic route to prepare salmeterol was applied.

Since α-haloketones react with primary amines in an unspecific way, which results in a complicated mixture of products,[33] secondary amine **5** was used in the reaction. This synthetic route was analogous to the one previously described in the literature,[34] except compound **2** was used instead of 5-(bromoacetyl)-2-hydroxybenzaldehyde (Scheme 3). Amine **5** reacted readily with **2** to give α-aminoketone **8**, which was further reduced to produce benzyl protected β-amino alcohol **9**. After removal of the protecting group and reduction of **10**, compound **1** was obtained, which was confirmed to be salmeterol by comparing its NMR spectra with literature data.[9,34,35]

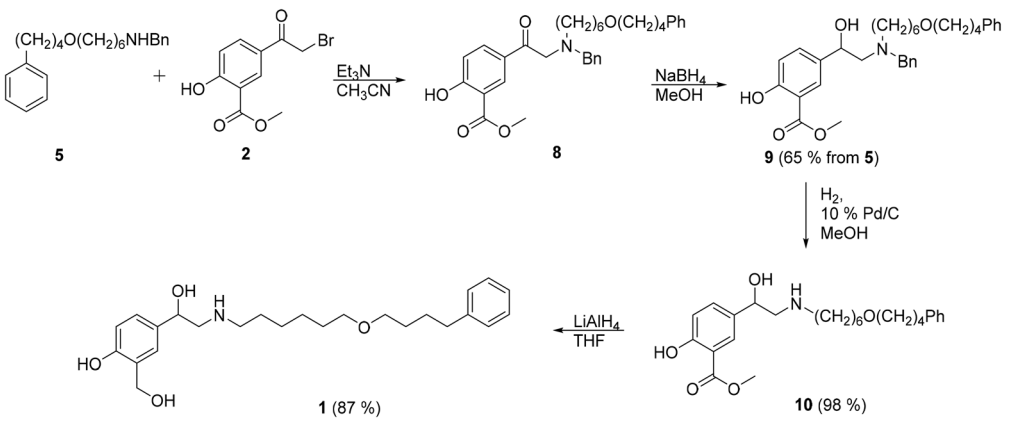

Scheme 3 Preparation of salmeterol (**1**).

The comparison of ^{1}H and ^{13}C NMR spectra of the obtained compounds **7** and **1** revealed that salmeterol and its isomer were synthesized, as indicated by MS analysis. Therefore, we analyzed compounds **6** and **10** with more NMR techniques in order to determine the structure of compound **6**. These compounds were selected for NMR analysis due to their higher solubility in the range of organic solvents, compared to reduced compounds **7** and **1**. Structures of two compounds were undoubtedly confirmed by 1D and 2D NMR spectra. Different proton and carbon chemical shifts of atoms near the amine group are clearly seen from the ^{1}H and APT NMR spectra (see ESI†) and approved by COSY, NOESY, HMQC and HMBC spectra. NOESY experiments have been shown as very useful in gaining more information about compounds **6** and **10**. The common NOE intramolecular interactions in both compounds are between the OCH_3 group and OH group on the phenyl ring and between the H-7 atom and phenyl atoms H-3 and H-5 (Fig. 3, ESI†). The two H-8 atoms in compound **10** are almost perpendicular to the phenyl ring plane thus showing NOE interactions with all phenyl proton atoms (H-3, H-5 and H-6), while in **6** the interaction with H-6 is missing. Long range interaction can be seen in **6** between H-8 and the OH group on atom C-1. Specific molecule conformation in the solvent allows these interactions through space.

To elucidate the reasons for the selectivity obtained in the reaction of β-halohydrin and amine, other primary amines (*n*-butylamine, $BuNH_2$ and *tert*-butylamine, *t*-$BuNH_2$) were first tested (Scheme 4). It was vital to see if the long-chain amine itself has any influence on the direction of the reaction since the synthesis of the amine is resource- and time-consuming.

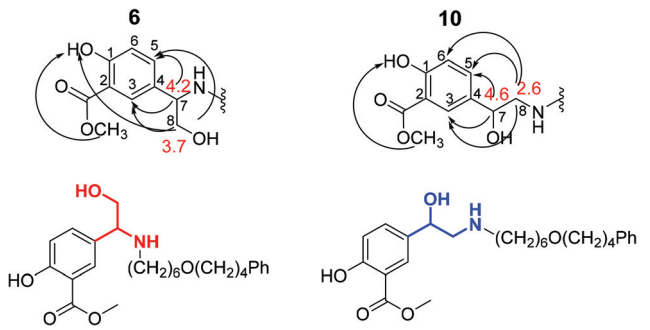

Fig. 3 NOE interaction (top) and molecular structures (bottom) of compounds **6** and **10**.

NMR spectra were used for differentiating isomers. In particular, the shifts of three hydrogen atoms between the hydroxyl and amino group in the ^{1}H NMR spectrum distinguished considerably for these two structural isomers. The difference is also notable for two corresponding signals in the ^{13}C NMR spectrum (ESI†). Primary amines $BuNH_2$ and *t*-$BuNH_2$ reacted the same as the long-chain amine used before and produced predominately compounds **11** and **12**, respectively. The lower regioselectivity of $BuNH_2$ is presumably the consequence of decreased steric effects of this nucleophile. Although $BuNH_2$ shows lower regioselectivity, it was used in further testing due to its availability and the fact that the steric effects of the nucleophile were minimized. Also, the result itself leaves room for improvement under other reaction conditions.

Since all primary amines reacted in the same way in the reaction, it was clear that the structure of aryl β-halohydrin played a dominant role in the direction of the reaction. As expected, when the reaction was performed with halohydrins without methyl salicylate moiety, the yield of the reaction was lower and the isomer ratio approached 1 : 1 (Scheme 5). Also, in the reactions with 2-bromo-1-phenylethanol (**15**) and methyl 3-(2-bromo-1-hydroxyethyl)benzoate (**16**), the corresponding epoxide was isolated in moderate yield (39% and 44% in reactions with **15** and **16**, respectively). This suggests that the possible reaction paths are *via* epoxides, which were formed and isolated under reaction conditions. When the reaction was performed with halohydrin **3**, the corresponding epoxide was not detected. It is also interesting to point out that the epoxide generated from benzyl protected compound **3** was previously used for the preparation of salmeterol.[36] The authors did not mention that another isomer was generated in the reaction (performed in THF). They also attempted the reaction with bromo alcohol as an electrophile, but a poor yield of the product was obtained.

Alkyl substituted epoxides are less dependent on reaction conditions and under basic conditions generate almost exclusively the α-alkyl-β-aminoethanol isomer *via* the S_N2 mechanism. However, aromatic epoxides are much more sensitive to reaction conditions due to the proximity of the aromatic ring which stabilizes the positive charge on the carbon atom next to it. Therefore, it seemed reasonable to test other reaction conditions for the halohydrin-amine reaction. To see if the reaction would proceed in the same way under different conditions, other solvents and bases were used in the reaction between bromo alcohol **3** and $BuNH_2$ (Table 1). The selected

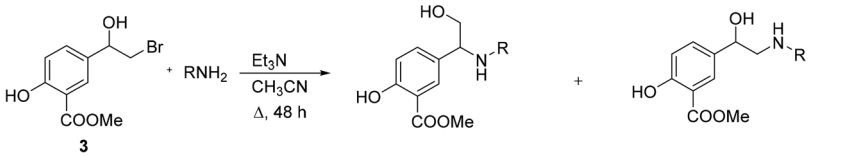

R = $(CH_2)_6O(CH_2)_4Ph$	80 %	**6**		R = $(CH_2)_6O(CH_2)_4Ph$	-	**10**
Bu	80 %	**11**		Bu	3 %	**13**
t-Bu	78 %	**12**		*t*-Bu	-	**14**

Scheme 4 The reaction of **3** with primary amines.

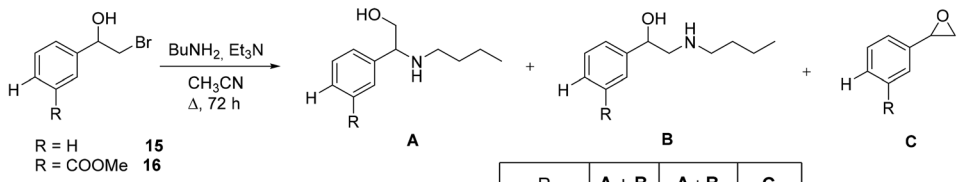

R	A + B	A : B	C
H	25 %	45 : 55	39 %
COOMe	49 %	30 : 70	44 %

Scheme 5 The reaction of aryl β-halohydrins and $BuNH_2$.

Table 1 The reaction of bromo alcohol **3** and $BuNH_2$ under different conditions[a]

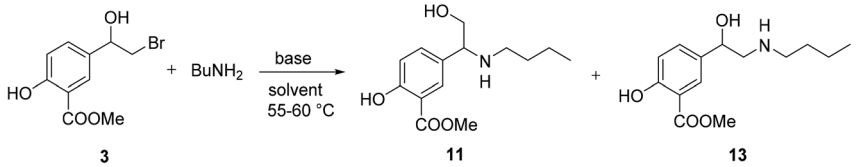

Entry	Solvent	Base	Time[b]/h	Yield/%	Ratio **11** : **13**[c]
1	Acetonitrile	Et_3N	48	83	96 : 4
2	THF	Et_3N	72	45	41 : 59
3	Toluene	Et_3N	72	38	63 : 37
4	Chloroform	Et_3N	72	82	82 : 18
5	Acetone	Et_3N	48	n.d.[d]	41 : 59
6	i-PrOH	Et_3N	48	90	100 : 0
7	$BuNH_2$	Et_3N	2	(43)[e]	(100 : 0)[e]
8	Acetonitrile	—	72	57	85 : 15
9	Acetonitrile	$BuNH_2$	24	93	82 : 18
10	Acetonitrile	Diethylaniline	72	56	86 : 14
11	Acetonitrile	DBU	2	<39[f]	100 : 0
12	Acetonitrile	K_2CO_3	2	(61)[g]	(100 : 0)[g]

[a] $BuNH_2$ (1.1 equiv.) was added to a solution of **3** (1 equiv.) in the corresponding solvent (10 mL per 1 mmol of **3**) followed by base (2 equiv.). [b] The reactions were processed when HPLC analysis indicated that **3** was no longer present in the reaction mixture or after 72 h. [c] Determined by NMR analysis of the obtained product. [d] Not determined due to an unidentified product present in the mixture in high portion. [e] The product is an amide formed from the corresponding ester. [f] An unidentified product is present in the mixture. [g] The product is the phenolic salt of **11**.

solvents included nonpolar (toluene, chloroform), moderately polar aprotic (THF), polar aprotic (acetone, acetonitrile) and polar protic solvents (i-PrOH, $BuNH_2$). To test the influence of the strength of the base in the reaction, diethylaniline was chosen as a weaker base then Et_3N, and DBU and K_2CO_3 were chosen as stronger organic and inorganic bases, respectively. Also, $BuNH_2$ was used as an example of primary instead of a tertiary amine, and the reaction was performed without the excess of the base. Since the reaction itself is rather slow, the temperature was kept in the range of 55–60 °C in all subsequent testings.

It is evident from the results (Table 1) that the solvent plays an important role in the direction of the reaction. Although it is clear that polar protic solvents favor isomer **11**, the influence of the polarity of the remaining solvents on the direction of the reaction is ambiguous. The reaction rate was rather low in toluene and chloroform, indicated by reactant **3** retrieved after chromatographic workup even after the reaction was performed for 72 hours. It must be stressed that the corresponding epoxide was not isolated in any of these reactions. Moreover, the course of the reaction in acetone was very unclear since one more product, with similar polarity on silica gel, is formed in the reaction, as indicated by the appearance of unknown peaks in the NMR spectrum of the product. When $BuNH_2$ was used as the solvent, the product was an amide that resulted from nucleophilic substitution of amine at the ester group on the aromatic ring. The best regioselectivity and yield was obtained in i-PrOH. Nevertheless, acetonitrile was used as a solvent when testing different organic bases in order to eliminate the possibility of a nucleophilic attack of i-PrOH on a substrate when stronger bases were tested.

The effect of different bases on the course of the reaction is more straightforward. Although stronger bases accelerate the reaction and direct it toward isomer 11, the yield of the reaction is reduced. This outcome is probably due to side reactions, which are frequent when strong bases are employed in

the combination with elevated temperature. Also, when an inorganic base was used, the obtained product was the phenolic salt of the product. When an excess base was not added or a weaker base was used, the 11 : 13 ratio was lower, as well as the reaction yield, with reactant 3 retrieved after the reaction. Again, corresponding epoxide was not isolated after the reaction. Although the reaction yield with a primary amine as the base was high, the 11 : 13 ratio was decreased compared to other bases. Thus, it is clear that the choice of base requires fine tuning – it should be rather strong, but not strong enough to promote side reactions.

Considering the obtained experimental results, we propose that the reaction between aromatic β-halohydrins and amines in basic conditions can take place through three reaction pathways (Scheme 6). The first two are well-established pathways – direct S_N2 substitution (pathway **I**) and reaction *via* epoxide intermediate (pathway **II**). The third pathway *via para*-quinone methide (pathway **III**) we introduce for the first time. Depending on the structure of the β-halohydrin moiety and the reaction conditions, one of these reaction pathways is predominant. In the vast majority of cases the reaction proceeds through the first two pathways. However, when a phenol is present in the structure of aromatic halohydrin, the formation of *para*-quinone methide intermediate (pathway **III**) is plausible. This reactive intermediate is then prone to nucleophilic addition under the above mentioned reaction conditions (Schemes 2 and 4).[37,38]

Besides the formation of β-aryl-β-amino alcohol isomer, there are other experimental indications that suggest the reaction does not proceed *via* conventional pathways. The phenol is efficiently deprotonated under reaction conditions, which is supported experimentally – in the case when K_2CO_3 was used as a base, the potassium salt of **11** was isolated as the product (Table 1). Also, the corresponding epoxide was not isolated in the case of bromo alcohol **3**, while it was a significant side product when bromo alcohols without an unprotected hydroxyl group on the phenyl ring were used. Furthermore, bromo alcohol **3** seems to be quite stable under milder basic conditions since it was isolated in cases when the reaction was not completed after 72 h. Finally, the combination of appropriate leaving group in the proximity of phenol, and the basic reaction conditions were reported to trigger the formation of *para*-quinone methides, both as stable products which can be isolated,[39–41] or as useful reactive intermediates.[42]

To support our hypothesis, we decided to turn to computational methods. First, we analyzed the nucleophilic attack of amine (methylamine) on our proposed *para*-quinone methide intermediate in acetonitrile and aimed to estimate the energy barrier (Fig. 4). As initial reactants in this reaction, complex of *para*-quinone methide and methylamine (***p*-QM:MeNH$_2$**) was optimized, harmonic analysis was performed, and the absence of imaginary frequencies was confirmed. The nitrogen in this minimum energy structure is 4.46 Å away from electrophilic C^β carbon atom in the vicinity of phenyl ring, and the ester group on the opposite part of the ring encloses the angle of −44.65° with the phenyl ring plane. The transition state has one normal mode with imaginary frequency (ν = 139.4i cm^{-1}). The displacement vectors clearly indicate that this is the mode leading to the intermediary product **IM^{III}A** (ESI†). C^β carbon atom is sp^2 hybridized, with small deviation of expected planarity (dihedral angle C3–C4–C7–H is −7.2°). From the point of view of the initial complex ***p*-QM:MeNH$_2$**, transition state **TS^{III}A** is only 5.9 kcal mol^{-1} higher in energy, while the intermediary product **IM^{III}A** is more stable for 13.7 kcal mol^{-1}. Final step leading to the reaction product **A** is the deprotonation of the amine and base-assisted hydrogen transfer to the phenyl oxygen. In the product, carboxylic group is again in the same plane with the phenyl ring, forming hydrogen bond with hydroxyl group from neighboring carbon atom. When calculations were performed in non-polar solvent (*n*-hexane), the

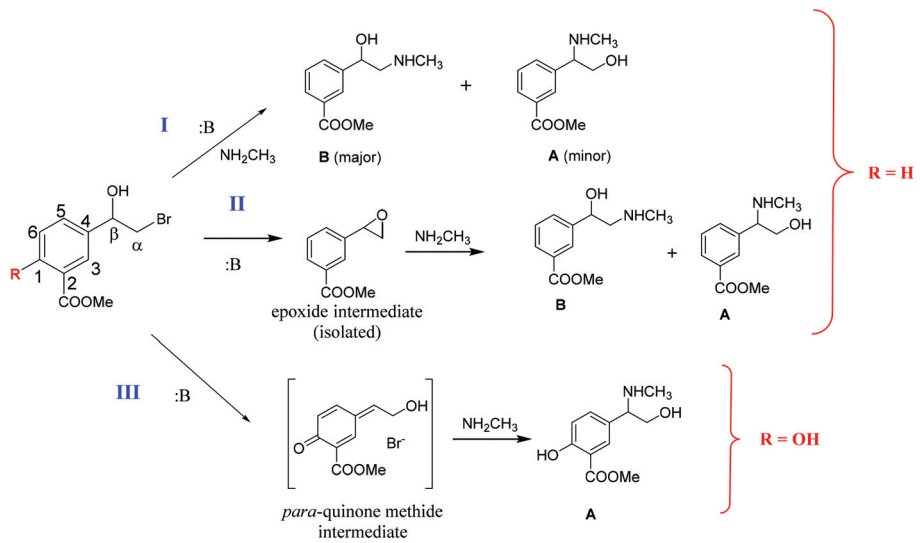

Scheme 6 Three possible reaction pathways between the aromatic bromo alcohol and an amine under basic conditions.

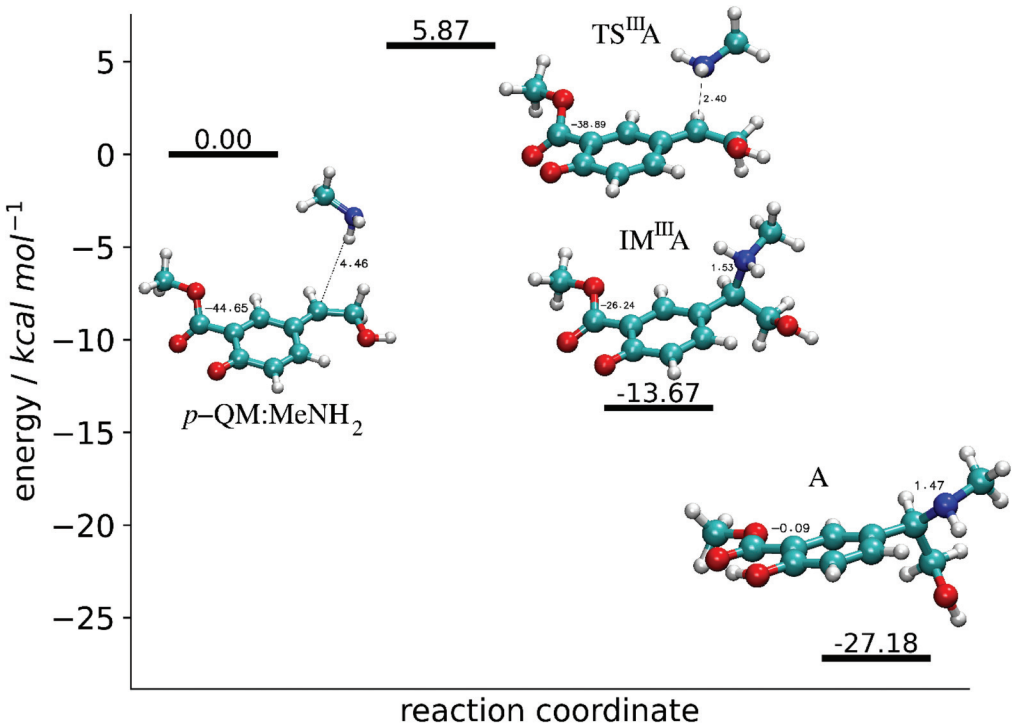

Fig. 4 The energy profile for half reaction from *para*-quinone methide – methylamine reaction complex to β-aryl-β-amino alcohol isomer. The relevant interatomic distances are in Angstrom, and the dihedral angle C3–C2–C–O is in degrees. B3LYP/aug-cc-pVDZ with SMD solvation model was used for geometry optimization, followed by B2-PLYP/aug-cc-pVTZ with SMD solvation model (solvent was acetonitrile) single point calculations.

estimated energy barrier for the attack of methyl amine on the C^{β} carbon atom of ***p*-QM:MeNH$_2$** was 12.2 kcal mol^{-1} (ESI†), which is more than twice the value obtained in acetonitrile. This indicates that the reaction in *n*-hexane is slower by four orders of magnitude, which is in agreement with our experimental findings.

Furthermore, we computed the reaction barrier for alternative classical mechanisms – pathways **I** and **II** in Scheme 6. The S_N2 reaction mechanism (Fig. 5), where direct attack of methylamine on the terminal carbon atom C^{α} occurs, leads toward expected product **B**. In the minimum energy complex of **3** and methylamine, the amine is 3.83 Å away from the terminal carbon. The transition state for the S_N2 mechanism is 17.3 kcal mol^{-1} higher in energy. It is characterized by sp^2 hybridized terminal carbon, while its neighborhood can be approximated by trigonal bipyramid, with leaving bromine and attacking methylamine on axial positions. Calculations for investigation of analogous mechanism, but with amine attacking the chiral carbon atom, resulted in interesting transition state. The bond between amine's nitrogen and C^{β} carbon is formed. Carbon atom remains in the center of the tetrahedron. Terminal carbon C^{α} to bromine distance of 2.52 Å indicates that bromine is leaving the molecule. But the most interesting part is transfer of the hydroxyl moiety from C^{β} toward terminal carbon atom, leading to the product **A**. The oxygen is closer to C^{α} (2.28 Å) than to the C^{β} (2.54 Å) carbon. This is corroborated by analysis of the displacement vectors of normal mode with imaginary frequency ν = 390.23i cm^{-1} (ESI†). This transition state is more than 73.3 kcal mol^{-1} higher in energy then the initial complex. The search for lower lying transition states for this mechanism failed. So, supposing that **3** is the dominant species in the solution and the reaction proceeds *via* S_N2 mechanism, the dominant product would be **B**, while due to the high barrier, **A** would not be isolated at all.

The second classical pathway is nucleophilic attack of the amine on the epoxide intermediate (epoxy-**3**) formed under basic conditions (Fig. 6, ESI†). According to our calculations, the products of this half reaction would be both isomers **A** and **B**, with expected **B** isomer in surplus. The expected isomer **B** is thermodynamically more stable than **A** by 4.1 kcal mol^{-1}, and the corresponding estimated barrier is lower by 1.6 kcal mol^{-1}. If this mechanism was dominant, the product ratio would be in disagreement with experimental observations. Furthermore, the analysis of analogous reaction pathway with compound **16** and methylamine shows similar energy profile (ESI†) which is in agreement with experimental results obtained for **16** (Scheme 5). This further corroborates the assumption that the presence of hydroxyl group on the aromatic ring in **3** directs the reaction towards different intermediate than in the case of **16**.

To summarize, the outcome of the reaction between the aryl β-halohydrin **3** and an amine is both solvent and base dependent, with the β-aryl-β-amino alcohol isomer being isolated in most cases. The outcome of the reaction cannot be explained by two conventional mechanisms – direct S_N2 or the

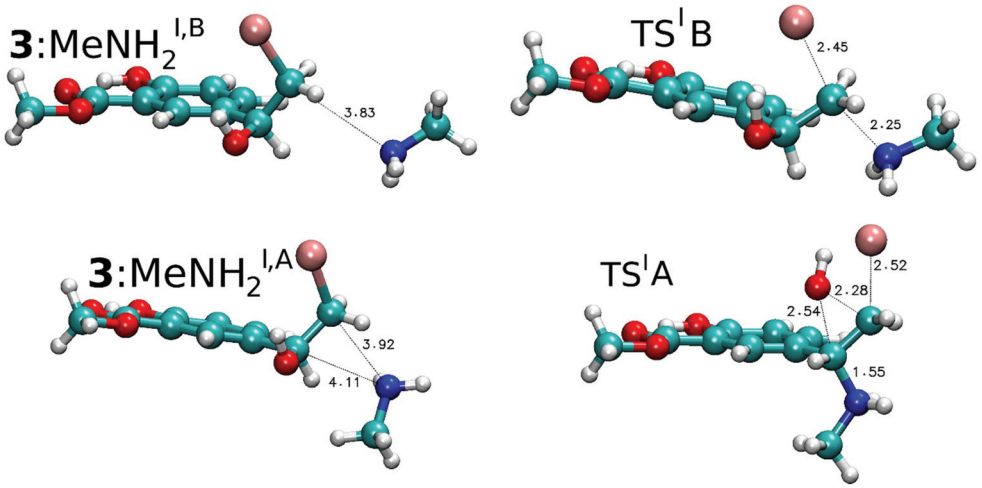

Fig. 5 Initial (left) and transition state (right) geometries relevant for S_N2 mechanism. Methylamine attacking terminal C^{α} (top) and C^{β} (bottom) carbon atom, with relevant distances in Angstrom.

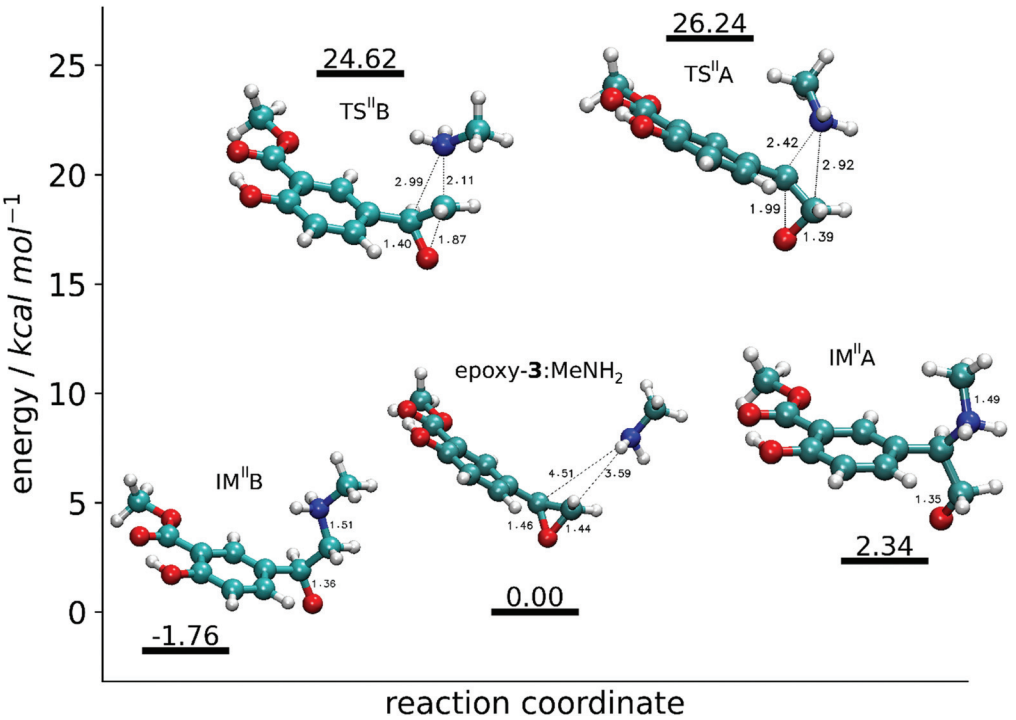

Fig. 6 The energy profile for half reaction from epoxide – methylamine reaction complex. The relevant interatomic distances are in Angstrom. B3LYP/aug-cc-pVDZ with SMD solvation model was used for geometry optimization, followed by B2-PLYP/aug-cc-pVTZ with SMD solvation model (solvent was acetonitrile) single point calculations.

epoxide pathway. We have shown that the barrier for concerted methylamine attack on C^{α} and leaving of bromine anion is around 17 kcal mol^{-1}, with expected final α-aryl-β-amino alcohol isomer, while the barrier for attack on C^{β} is significantly higher. On the other hand, the estimated barriers for methylamine attack on C^{α} and C^{β} of the corresponding epoxide are very close in energy. The estimated barrier of 1.6 kcal mol^{-1} leads to a reaction rate difference of 1 : 11.5 at a temperature of 330 K. Thus, the expected product **B** is both thermodynamically and kinetically favored. The presence of *para*-quinone methide intermediate with sp^2 hybridized C^{β} atom prone to the attack by amine results exclusively in **A**-like product, *i.e.* β-aryl-β-amino alcohol, and fully explains the regioselectivity observed experimentally.

Finally, we were able to synthesize two isomers of the saligenin class of β2-agonists bronchodilators. The isomer of sal-

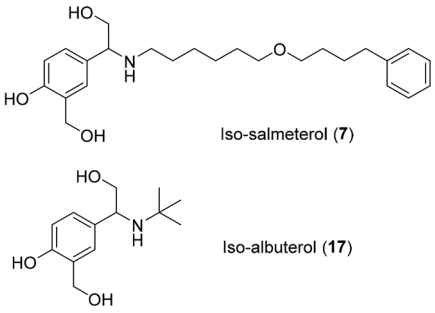

Fig. 7 Isomers of saligenin type β2-agonist bronchodilators.

meterol is compound **7**, and the reduction of compound **12** afforded **17**, the isomer of albuterol (Fig. 7). These isomers were tested for inhibition of acetylcholinesterase (AChE; EC 3.1.1.7) and butyrylcholinesterase (BChE; E.C. 3.1.1.8) since in our earlier paper[30] we demonstrated that albuterol and salmeterol can reduce human cholinesterase activity. Since the efficacy of compound that targets BChE activity can be affected by the human BChE gene polymorphism,[11,30] inhibition activity was tested towards two BChE variants with different catalytic properties, usual BChE (hydrolyzes certain short-acting neuromuscular blocking agents widely used during anesthesia, *i.e.* succinylcholine and mivacurium) and atypical BChE (cannot hydrolyze succynilcholine).

Kinetic studies revealed that iso-albuterol and iso-salmeterol reversibly inhibited all of the tested cholineaterases with enzyme-inhibitor dissociation constants ($K_{(I)}$) ranging between 2.6 μM and 1.3 mM (Table 2) classifying these compounds as low-potency inhibitors.[43] The highest inhibition potency was displayed by iso-salmetrol toward usual BChE, while the lowest was that of iso-albuterol toward AChE. The inhibition potency of iso-salmetrol was 40–80 times higher than that of iso-albuterol, which could have been due to the elongation of the *tert*-butylamino group, as it is in iso-albuterol, to phenylbutoxyhexylamino group present in iso-salmeterol. Both compounds are seven times more potent inhibitors of BChE than of AChE, meaning that both compounds can be considered as selective BChE inhibitors. The approximately five-fold decrease of inhibition potency toward atypical BChE compared to usual BChE could have been a consequence of the point mutation of aspartate 70 to glycine (D70G), a residue located in the peripheral site of the active centre of BChE and close to the entrance of the active centre gorge. The D70G mutant was confirmed to have a different conformation compared to usual BChE, particularly affecting the tryptophane 82 that participates in accepting the ligand and its proper orientation at the entry of the active site of the BChE.[44]

Table 2 Reversible inhibition of cholinesterases by bronchodilating β2-agonists bearing the saligenin structure

	$K_{(I)}$ [a]/mM		
	AChE	Usual BChE	Atypical BChE
Iso-albuterol (**17**)	1.3 ± 0.2	0.17 ± 0.02	0.69 ± 0.13
Iso-salmeterol (**7**)	0.016 ± 0.003	0.0026 ± 0.0003	0.017 ± 0.002
Albuterol[30]	2.0 ± 0.2	0.071 ± 0.006	1.4 ± 0.2
Salmeterol[30]	0.030 ± 0.002	0.013 ± 0.001	0.086 ± 0.018

[a] The enzyme-inhibitor complex dissociation constant ($K_{(I)}$ ± SE) was determined by linear regression from $K_{i,app}$ constants obtained from at least two experiments.

Generally speaking, the inhibition profile of the tested isomers and cholinesterases is similar to that reported for albuterol and salmeterol; inhibition potency is lower toward AChE compared to BChE and the highest inhibition potency is that for usual BChE. When the inhibition potency of isomers is compared to that of corresponding bronchodilators, isomers are 2–5 times more potent inhibitors. It seems that structural rearrangements of the hydroxyl group in the alkyl chain on the benzene ring, as in isomers of albuterol and salmeterol, can ensure an orientation in the active site of a cholinesterase that is more favourable for inhibition compared to that of the corresponding bronchodilators. The exception is the inhibition of usual BChE by iso-albuterol, which was twice less potent compared to that by albuterol suggesting that rearrangement of the hydroxyl groups present in albuterol is more optimal for inhibition.

3. Conclusion

We developed two synthetic routes that enable preparation of both saligenin-based β2-agonists, albuterol and salmeterol, and their isomers, iso-albuterol and iso-salmeterol. All products are obtained in high yield starting from methyl 5-acetylsalicylate. HRMS analysis confirmed that the prepared compounds are isomers, while 1D and 2D NMR were used for determining the structure of the prepared isomers. The obtained structural isomers contain β-aryl-β-aminoethanol moiety opposed to the substituted α-aryl-β-aminoethanol structure found in common β2-adenoreceptor agonists. The study of the halohydrin-amine reaction, responsible for the formation of the isomer, revealed that the methyl salicylate moiety in the structure of β-halohydrin dictates the reaction path, while the effect of the used primary amine is negligible. Also, the solvent plays a relevant role in the direction of the reaction with polar protic solvents favoring the unexpected isomer in the reaction. On the other hand, the base has more straightforward effect on the rate of the reaction and on the products' isomer ratio. Fine tuning of the base strength is essential for adequate reaction yield and isomer ratio, since strong bases lower the yield, while weaker bases increase reaction time and shift isomer ratio toward expected isomer. The most probable reaction path in the presence of the strong base, *via para*-quinone methide intermediate, is corroborated by quantum chemistry calculations. This is in accordance with experimental findings, and explains the influence of base strength, both on reaction mechanism and reaction outcome. Since we successfully obtained isomers of albuterol and salmeterol, the inhibition potency of iso-albuterol and iso-salmeterol

toward human acetylcholinesterase (AChE) and usual and atypical butyrylcholinesterase (BChE) was tested and compared to the inhibition potency of common saligenin-based β2-agonists. Kinetic studies demonstrated that both isomers are low-potency reversible inhibitors of human cholinesterases with an approximately seven times higher preference toward BChE compared to AChE.

4. Experimental section

4.1. Chemistry

4.1.1. General considerations. All of the reactions were conducted under an argon atmosphere unless otherwise noted. THF was distilled from lithium aluminum hydride. All of the other reagents and solvents were purchased from commercial sources and used without purification. TLC was performed on aluminium backed silica plates (60 F254, Merck). UV light (254 nm) or phosphomolibdic acid reagent were used for visualizing. Column chromatography was performed on silica gel (Silica Gel 60, 70–230 mesh, Fluka). ^{1}H and ^{13}C NMR were recorded on a Bruker AV 300 spectrometer, while COSY, NOESY, HMQC and HMBC spectra were recorded on a Bruker AV 600 spectrometer. The NOESY spectra were measured in a phase-sensitive mode, with a mixing time of 0.90 s and 32 scans per each increment. The spectral width was 9615.38 Hz, 2048 points in the F2 dimension and 512 increments in the F1 dimension, subsequently zero-filled to 1024 points. The resulting FID resolution was 4.69 Hz per point and 18.75 Hz per point in the F2 and F1 dimensions, respectively. Chemical shifts (δH and δC) are quoted in parts per million (ppm), referenced to TMS. HPLC measurements were done using a Shimadzu 10A VP HPLC system. Nucleosil 100-5 C18, 250 mm × 4.6 mm column, A: H_2O, MeOH, H_3PO_4 (85%) = 90 : 10 : 0.5, B: MeOH, Gradient method: 10/100/100/10%B in 0/20/25/27 min, 1 mL min^{-1}, 220 nm. The LC/MS system consisted of an Agilent Technologies 1200 Series HPLC instrument and Agilent Technologies 6420 Triple Quad LC/MS equipped with electrospray ion source. High resolution mass spectrometry (HRMS) was performed on a 4800 Plus MALDI TOF/TOF Analyzer. [4-(6-Bromo-hexyloxy)-butyl]-benzene,[34] methyl 5-(bromoacetyl)-salicylate (**2**)[32] and *N*-benzyl-6-(4-phenylbutoxy)-1-hexanamine (**5**)[34] were prepared according to known procedures.

4.1.2. Synthesis of amine and β-halohydrin

*Methyl 5-(2-bromo-1-hydroxy-ethyl)-salicylate (**3**).* Methyl 5-(bromoacetyl)salicylate (0.70 g, 2.6 mmol) was suspended in MeOH (25 mL) and the mixture was cooled to 0 °C. Sodium borohydride (99 mg, 2.6 mmol) was added in several portions. After addition the reaction mixture was stirred at room temperature for 1 hour. The solvent was evaporated and saturated aqueous NH_4Cl solution (15 mL) was added to the resulting white solid and extracted with DCM (3 times). The combined organic extracts were washed with water, dried over Na_2SO_4 and concentrated under reduced pressure to afford a colourless oil. The crude product was purified by silica gel column chromatography (DCM, R_f = 0.25) to give a colourless oil which crystallizes (0.64 g, 91%).

^{1}H NMR (300 MHz, $CDCl_3$) δ 10.77 (1H, s), 7.87 (1H, d, J = 2.3 Hz), 7.47 (1H, dd, J = 8.5, 2.3 Hz), 6.99 (1H, d, J = 8.5 Hz), 4.87 (1H, dt, J = 8.7, 2.8 Hz), 3.95 (3H, s), 3.60 (1H, dd, J = 10.4, 3.6 Hz), 3.51 (1H, dd, J = 10.4, 8.7 Hz), 2.69 (1H, d, J = 2.8 Hz); ^{13}C NMR (75 MHz, $CDCl_3$) δ 170.30, 161.66, 133.41, 131.19, 127.61, 118.10, 112.39, 73.08, 52.49, 40.09. HRMS (ESI-TOF) m/z: $[M + Na]^+$ calcd for $C_{13}H_{20}NO_3Na$ 261.1341; found 261.1350.

*6-(4-Phenyl-butoxy)-hexylamine (**4**).* Potassium phthalimide (0.65 g, 3.5 mmol) was added to a solution of [4-(6-bromo-hexyloxy)-butyl]-benzene (1.00 g, 3.2 mmol) in DMF (10 mL). The reaction mixture was stirred at 60 °C for 2 hours. After cooling to room temperature water (10 mL) was added and extracted with diethyl ether (3 times). The combined organic extracts were extracted with saturated aqueous $NaHCO_3$ solution, washed with water, dried over Na_2SO_4 and concentrated under reduced pressure to afford a colourless oil. The oil was dissolved in EtOH (15 mL) and hydrazine hydrate (50–60%, 0.3 mL) was added. The reaction mixture was refluxed for 1.5 hours. The solvent was evaporated and diethyl ether was added to the white residue. The mixture was filtered and white solid washed with diethyl ether. The filtrate was concentrated under reduced pressure to give colourless oil (0.75 g, 92%).[45]

^{1}H NMR (300 MHz, $CDCl_3$) δ 7.30–7.23 (2H, m), 7.20–7.15 (3H, m), 3.43–3.35 (4H, m), 2.74–2.67 (2H, m), 2.66–2.59 (2H, m), 2.55 (2H, br s), 1.72–1.42 (8H, m), 1.40–1.30 (4H, m); ^{13}C NMR (75 MHz, $CDCl_3$) δ 142.51, 128.42, 128.26, 125.67, 70.85, 70.71, 41.84, 35.74, 32.96, 29.71, 29.41, 28.09, 26.72, 26.04; MS/+ESI (m/z): 150.3 ($[C_{16}H_{27}NO + H]^+$).

4.1.3. Synthesis of salmeterol (1). The synthesis was analogous to that described in literature,[34] apart from using methyl 5-(bromoacetyl)-salicylate as an electrophile.

*Methyl 5-(2-{benzyl-[6-(4-phenyl-butoxy)-hexyl]-amino}-1-hydroxy-ethyl)-salicylate (**9**).* To a solution of **2** (0.61 g, 2.2 mmol) in acetonitrile (10 mL), the solution of **5** (0.76 g, 2.2 mmol) in acetonitrile (15 mL) was added dropwise under inert atmosphere. Triethylamine (0.62 mL, 4.4 mmol) was added dropwise and the reaction mixture was stirred at room temperature for 40 min. The solvent was evaporated, DCM (25 mL) added to the resulting yellow residue and washed with water. The organic layer was dried over Na_2SO_4 and concentrated under reduced pressure to give a yellow oil. Further purification of gained product **8** was unsuccessful, therefore the second reaction step was performed with crude product.

The solution of obtained oil (1.38 g) in MeOH (35 mL) was cooled in ice bath and sodium borohydride (100 mg, 2.6 mmol) was added in several portions. After addition, the reaction mixture was stirred at room temperature for 1 hour. The solvent was evaporated and water (15 mL) was added to the resulting white solid and extracted with DCM (3 times). The combined organic extracts were dried over Na_2SO_4 and concentrated under reduced pressure to afford a yellow residue. The crude product was purified by silica gel column chromatography (DCM–MeOH, 50 : 1 to 20 : 1, R_f = 0.64 for 20 : 1) to give a colourless oil (0.77 g, 65%).

^{1}H NMR (300 MHz, $CDCl_3$) δ 10.69 (1H, s), 7.78 (1H, d, J = 2.1 Hz), 7.38–7.23 (8H, m), 7.19–7.15 (3H, m), 6.94 (1H, d, J = 8.6 Hz), 4.58 (1H, dd, J = 10.0, 3.7 Hz), 3.93 (3H, s), 3.88 (1H, d, J = 13.4 Hz), 3.49 (1H, d, J = 13.4 Hz), 3.39 (4H, m), 2.66–2.40 (6H, m), 1.71–1.48 (9H, m), 1.34–1.25 (4H, m); ^{13}C NMR (75 MHz, $CDCl_3$) δ 170.58, 161.05, 142.58, 138.62, 133.53, 133.14, 129.08, 128.52, 128.49, 128.33, 127.35, 125.75, 117.67, 112.10, 70.91, 70.80, 68.82, 62.55, 58.65, 53.89, 52.31, 35.82, 29.80, 29.49, 28.16, 27.23, 26.95, 26.17.

*Methyl 5-{2-[6-(4-phenyl-butoxy)-hexylamino]-1-hydroxy-ethyl}-salicylate (**10**).* Bn protected aminoalcohol **9** (0.23 g, 0.43 mmol) was dissolved in MeOH (8 mL) and hydrogenated in the presence of 10% Pd–C (30 mg) for 2 hours. The catalyst was filtered over a Celite pad and the filtrate was evaporated under reduced pressure to afford a colourless oil which crystallizes (0.19 g, 98%).

^{1}H NMR (300 MHz, $CDCl_3$) δ 7.84 (1H, d, J = 2.1 Hz), 7.45 (1H, dd, J = 8.6, 2.1 Hz), 7.28–7.25 (2H, m), 7.18–7.15 (3H, m), 6.96 (1H, d, J = 8.6 Hz), 4.68 (1H, dd, J = 9.3, 3.3 Hz), 3.94 (3H, s), 3.41 (2H, t, J = 6.4 Hz), 3.38 (2H, t, J = 6.7 Hz), 2.86 (1H, dd, J = 12.2, 3.3 Hz), 2.72–2.65 (2H, m), 2.65–2.61 (3H, m), 1.71–1.64 (2H, m), 1.63–1.59 (2H, m), 1.57–1.48 (4H, m), 1.37–1.32 (4H, m); ^{13}C NMR (75 MHz, $CDCl_3$) δ 170.53, 161.10, 142.57, 133.46, 133.35, 128.47, 128.32, 127.26, 125.74, 117.72, 112.17, 70.88, 70.80, 70.72, 56.96, 52.32, 49.39, 35.80, 29.83, 29.76, 29.47, 28.14, 27.10, 26.15; MS/+ESI (m/z): 444.4 ($[C_{26}H_{37}NO_5 + H]^+$).

*Salmeterol (**1**).* Lithium aluminum hydride (50 mg) was suspended in dry diethyl ether (3 mL) in inert atmosphere. The solution of ester **10** (0.31 g, 0.69 mmol) in dry diethyl ether (8 mL) was added dropwise. The reaction mixture was stirred at room temperature for 1 hour. The reaction was quenched with a few drops of water followed by the addition of EtOH (5 mL) and saturated aqueous solution of Rochelle salt (10 mL). The layers were separated and the aqueous phase washed three times with EtOAc. The combined organic extracts were dried over Na_2SO_4 and concentrated under reduced pressure. The product precipitated in cold EtOAc to give an off-white solid (0.25 g, 87%).

^{1}H NMR (300 MHz, $CDCl_3$) δ 7.33–7.25 (2H, m), 7.22–7.16 (3H, m), 7.06 (1H, d, J = 8.1 Hz), 6.92 (1H, s), 6.76 (1H, d, J = 8.1 Hz), 4.69 (2H, s), 4.56–4.41 (4H, m), 3.47–3.36 (4H, m), 2.70–2.47 (6H, m), 1.74–1.40 (8H, m), 1.37–1.26 (4H, m); ^{13}C NMR (75 MHz, $CDCl_3$) δ 155.80, 142.54, 133.66, 128.49, 128.34, 126.59, 125.97, 125.76, 125.63, 116.38, 71.49, 70.95, 70.84, 63.45, 56.70, 49.40, 35.80, 29.70, 29.63, 29.42, 28.11, 27.14, 26.13.

4.1.4. Reactions of methyl 5-(2-bromo-1-hydroxy-ethyl)-salicylate with amines

General procedure. The corresponding amine (1 equiv.) was added dropwise under inert atmosphere to a solution of **3** (1 equiv.) in acetonitrile (10 mL per 1 mmol of bromide). Triethylamine (2 equiv.) was added dropwise and the reaction mixture was stirred at 55 °C (45 °C in the case of *tert*-butylamine) for 48 hours. The solvent was evaporated and the obtained residue purified by silica gel column chromatography (DCM–MeOH, 20 : 1 to 9 : 1) to afford the product.

*Methyl 5-{2-hydroxy-1-[6-(4-phenyl-butoxy)-hexylamino]-ethyl}-salicylate (**6**).* Yellow oil (0.35 g, 80%) starting from **3** (0.28 g). R_f = 0.42 (DCM–MeOH, 9 : 1).

^{1}H NMR (300 MHz, $CDCl_3$) δ 7.99 (1H, d, J = 2.3 Hz), 7.77 (1H, dd, J = 8.6, 2.3 Hz), 7.32–7.25 (2H, m), 7.21–7.16 (3H, m), 7.07 (1H, d, J = 8.6 Hz), 4.32–4.25 (1H, m), 4.14–4.05 (1H, m), 3.99 (3H, s), 3.98–3.90 (1H, m), 3.39 (2H, t, J = 6.3 Hz), 3.35 (2H, t, J = 6.5 Hz), 2.75–2.67 (2H, m), 2.63 (2H, t, J = 7.3 Hz), 1.83–1.73 (2H, m), 1.70–1.49 (6H, m), 1.36–1.26 (4H, m); ^{13}C NMR (75 MHz, $CDCl_3$) δ 170.02, 162.08, 142.44, 135.18, 130.16, 128.40, 128.26, 125.68, 125.12, 118.86, 112.75, 70.73, 70.64, 64.28, 64.09, 52.56, 46.35, 35.71, 29.55, 29.34, 28.01, 27.28, 26.78, 25.76; MS/+ESI (m/z): 444.4 ($[C_{26}H_{37}NO_5 + H]^+$).

*Methyl 5-(1-butylamino-2-hydroxy-ethyl)-salicylate (**11**).* Yellow oil (83 mg, 83%) starting from **3** (103 mg). R_f = 0.40 (DCM–MeOH, 9 : 1). The product containes 3% of isomer **13** (determined by NMR).

^{1}H NMR (300 MHz, $CDCl_3$) δ 7.99 (1H, d, J = 2.2 Hz), 7.78 (1H, dd, J = 8.6, 2.2 Hz), 7.05 (1H, d, J = 8.6 Hz), 4.32 (1H, m), 4.13 (1H, m), 3.97 (3H, s), 3.96–3.91 (1H, m), 2.71 (2H, m), 1.76 (2H, m), 1.37–1.25 (2H, m), 0.86 (3H, t, J = 7.4 Hz); ^{13}C NMR (75 MHz, $CDCl_3$) δ 170.06, 162.26, 135.30, 130.37, 124.67, 119.01, 112.90, 64.27, 64.20, 52.63, 46.18, 29.17, 20.18, 13.63; MS/+ESI (m/z): 268.2 ($[C_{14}H_{21}NO_4 + H]^+$).

*Methyl 5-(1-tert-butylamino-2-hydroxy-ethyl)-salicylate (**12**).* Yellow oil (166 mg, 78%) starting from **3** (219 mg). R_f = 0.37 (DCM–MeOH, 9 : 1).

^{1}H NMR (300 MHz, $CDCl_3$) δ 8.04 (1H, d, J = 2.3 Hz), 7.87 (1H, dd, J = 8.7, 2.3 Hz), 7.04 (1H, d, J = 8.7 Hz), 4.39 (1H, dd, J = 9.1, 3.8 Hz), 4.03 (1H, dd, J = 12.1, 9.1 Hz), 3.97 (3H, s), 3.79 (1H, dd, J = 12.1, 3.8 Hz), 1.32 (9H, s); ^{13}C NMR (75 MHz, $CDCl_3$) δ 169.98, 161.97, 135.35, 129.86, 126.75, 118.80, 112.74, 64.70, 61.06, 58.14, 52.58, 28.29; MS/+ESI (m/z): 268.2 ($[C_{14}H_{21}NO_4 + H]^+$).

4.1.5. Reaction of *n*-butylamine with other halohydrins.

The reactions of 2-bromo-1-phenylethanol (**15**) and methyl 3-(2-bromo-1-hydroxyethyl)benzoate (**16**) with *n*-butylamine were conducted according to the above presented reaction conditions.

4.1.6. Testing different base/solvent conditions.

N-Butylamine (1.1 equiv.) was added dropwise under inert atmosphere to a solution of **3** (1 equiv.) in solvent according to Table 2 (10 mL per 1 mmol of bromide). The corresponding base (2 equiv.) was added dropwise and the reaction mixture was stirred at 55–60 °C until the completion of reaction (monitored by HPLC) or for 72 hours. The solvent was evaporated and the obtained residue purified by silica gel column chromatography (DCM–MeOH, 20 : 1 to 9 : 1) to afford the product. The product was analysed by ^{1}H NMR spectroscopy to determine the **11** : **13** ratio.

N-Butyl-5-(1-butylamino-2-hydroxyethyl)-2-hydroxy-benzamide (Table 2, entry 7). Yellow oil (49 mg, 43%) obtained after reaction in $BuNH_2$, starting from **3** (102 mg). R_f = 0.35 (DCM–MeOH, 9 : 1).

^{1}H NMR (300 MHz, $CDCl_3$) δ 8.56 (1H, s), 7.73 (1H, t, J = 5.3 Hz), 7.35 (1H, dd, J = 8.5, 1.3 Hz), 6.97 (1H, d, J = 8.5 Hz), 4.38

(1H, dd, J = 9.2, 3.6 Hz), 4.23 (1H, dd, J = 12.2, 9.2 Hz), 4.05 (1H, dd, J = 12.2, 3.6 Hz), 3.43 (2H, q, J = 6.4 Hz), 2.82 (2H, t, J = 8.0 Hz), 1.81 (2H, m), 1.67 (2H, m), 1.46–1.25 (4H, m), 0.92 (3H, t, J = 7.3 Hz), 0.86 (3H, t, J = 7.4 Hz); ^{13}C NMR (75 MHz, $CDCl_3$) δ 169.53, 162.86, 134.42, 126.58, 120.76, 119.34, 115.68, 64.86, 63.57, 46.05, 39.82, 31.42, 28.09, 20.38, 20.05, 13.87, 13.56; MS/+ESI (m/z): 309.2 ($[C_{17}H_{28}N_2O_3 + H]^+$).

Potassium 4-(1-butylamino-2-hydroxyethyl)-2-methoxycarbonylphenolate (Table 2, entry 12). Yellow solid (68 mg, 61%) obtained after reaction with K_2CO_3 as the base, starting from **3** (100 mg). R_f = 0.20 (DCM–MeOH, 9 : 1).

^{1}H NMR (300 MHz, $CDCl_3$) δ 7.76 (1H, d, J = 2.2 Hz), 7.41 (1H, dd, J = 8.6, 2.2 Hz), 6.96 (1H, d, J = 8.6 Hz), 3.94 (3H, s), 3.75–3.64 (2H, m), 3.58–3.50 (1H, m), 2.48 (2H, m), 1.50–1.40 (2H, m), 1.37–1.23 (2H, m), 0.87 (3H, t, J = 7.3 Hz); ^{13}C NMR (75 MHz, $CDCl_3$) δ 170.51, 161.18, 134.72, 131.45, 128.66, 118.06, 112.42, 66.48, 63.89, 52.45, 47.08, 32.24, 20.48, 14.04; MS/+ESI (m/z): 268.2 ($[C_{14}H_{21}NO_4 + H]^+$); MS/−ESI (m/z): 265.9 ($[C_{14}H_{20}NO_4]^-$).

4.1.7. Reduction of prepared methyl aminoalcohol salicylates

General procedure. Lithium aluminum hydride (1 equiv.) was suspended in dry THF (4 mL per 1 mmol of ester) in inert atmosphere. The solution of the corresponding ester (1 equiv.) in dry THF (8 mL per 1 mmol of ester) was added dropwise. The reaction mixture was stirred at room temperature for 1 hour. The reaction was quenched with a few drops of water followed by the addition of EtOH and saturated aqueous solution of Rochelle salt. After stirring for 1 hour, EtOAc was added. The layers were separated and the aqueous phase washed two times with EtOAc. The combined organic extracts were dried over Na_2SO_4 and concentrated under reduced pressure.

Iso-salmeterol (7). Off-white viscous oil which crystallizes upon standing (0.219 g, 80%) starting from **6** (0.292 g). Purified by column chromatography in DCM–MeOH, 9 : 1 + 1% Et_3N (R_f = 0.21). mp 36–37 °C.

^{1}H NMR (300 MHz, $CDCl_3$) δ 7.28–7.24 (2H, m), 7.18–7.14 (3H, m), 7.03 (1H, dd, J = 7.9, 1.7 Hz), 6.99 (1H, s), 6.78 (1H, d, J = 7.9 Hz), 4.72 (2H, s), 4.45 (3H, br s), 3.66–3.59 (2H, m), 3.54–3.49 (1H, m), 3.40 (2H, t, J = 6.6 Hz), 3.35 (2H, t, J = 6.6 Hz), 2.62 (2H, t, J = 7.5 Hz), 2.52–2.41 (2H, m), 1.70–1.63 (2H, m), 1.63–1.57 (2H, m), 1.53–1.42 (4H, m), 1.29–1.23 (4H, m); ^{13}C NMR (75 MHz, $CDCl_3$) δ 155.79, 142.53, 131.04, 128.48, 128.35, 128.28, 126.86, 126.03, 125.77, 116.55, 70.94, 70.83, 66.06, 63.92, 63.58, 47.19, 35.79, 29.68, 29.58, 29.40, 28.07, 27.08, 26.05. HRMS (MALDI TOF/TOF) m/z: $[M + H]^+$ calcd for $C_{25}H_{37}NO_4$ 416.2801; found 416.2810.

Iso-albuterol (17). Yellow solid (92 mg, 64%) starting from **12** (160 mg). Purified by recrystallization from diisopropyl ether. mp 51–52 °C.

^{1}H NMR (300 MHz, DMSO) δ 7.25 (1H, s), 7.03 (1H, d, J = 8.2 Hz), 6.65 (1H, d, J = 8.2 Hz), 4.45 (2H, s), 3.70 (1H, m), 3.27 (1H, m), 3.07 (1H, m), 0.92 (9H, s); ^{13}C NMR (75 MHz, DMSO) δ 152.66, 135.20, 127.66, 126.15, 125.93, 114.03, 67.28, 58.78, 58.46, 50.52, 30.01. HRMS (MALDI TOF/TOF) m/z: $[M + H]^+$ calcd for $C_{13}H_{21}NO_3$ 240.1600; found 240.1604.

4.2. Computational details

All structures were optimized using B3LYP hybrid functional[46] and Dunning's correlation consistent basis sets augmented with diffuse functions (aug-cc-pVDZ).[47] Solvation effects were incorporated using Truhlar's SMD solvation model,[48] while the solvent was acetonitrile (ε_r = 35.688). For each structure the harmonic vibrational analysis was performed, to properly identify the nature of the optimized structures. Single point calculations for all relevant structures were performed with double hybrid B2-PLYP functional[49] combined with Grimme's D3BJ dispersion[50,51] and triple zeta valence quality basis set (aug-cc-pVTZ). Solvent effects were included in geometry optimization and frequency calculations, as well as in all single point energy calculations. For all calculations Gaussian 16[52] was used.

4.3. Enzyme inhibition

Human native serum was used as a source of BChE, while recombinant human AChE was used as a source of AChE. BChE variants were confirmed earlier as described previously.[53] The usual BChE was collected from female donors at the Institute for Medical Research and Occupational Health, Zagreb, Croatia (IMROH) and the atypical BChE was a gift from Dr Oksana Lockridge (University of Nebraska Medical Centre, Eppley Institute, Omaha, USA). Recombinant human AChE was a gift from Dr Florian Nachon (Département de Toxicologie, IRBA, France). Enzyme dilutions were done in phosphate buffer and those of recombinant AChE with the addition of 0.01% BSA. This study was reviewed and approved by the IMROH Ethics Committee. Iso-albuterol was dissolved in water and iso-salmeterol in ethanol. All further dilutions were done in water. All of the experiments were done in 0.1 M phosphate buffer, pH 7.4 at 25 °C, the Tecan Infinite M200PRO plate reader (Tecan, Austria, GmbH, Salzburg, Austria). The inhibition mixture (300 μL final) contained a buffer, enzyme, DTNB (0.33 mM final) and inhibitor, and after the addition of the substrate, the activity was assayed by Ellman's method[54] as described earlier.[55] Acetylthiocholine (ATCh) was used as a substrate for AChE and propyonylthiocholine (PTCh) as a substrate for BChE. Baseline activity was determined in the presence of water since the proportion of ethanol in AChE and BChE activity measurement was up to 0.012% and 0.03%, respectively, which does not affect enzyme activity. The inhibition potency of the compounds was determined as a dissociation constant for an enzyme-inhibitor complex, $K_{(I)}$, evaluated from the impact of substrate concentrations [S] on the degree of inhibition applying the Hunter–Downs equation.[56] Detailed description in ref. 55

$$K_{i,app} = \frac{v_i}{v_0 - v_i} \cdot [I] = K_{(I)} + \frac{K_{(I)}}{K_{(S)}} \cdot [S]$$

where $K_{i,app}$ is an apparent enzyme-reversible inhibitor complex dissociation constant obtained at a given substrate concentration [S] in the presence of inhibitor concentration [I] and calculated from the enzyme activities v_0 and v_i measured

without inhibitor and in the presence of inhibitor concentration [I], respectively.[55]

Conflicts of interest

There are no conflicts of interest to declare.

Acknowledgements

The authors gratefully acknowledge Vladimir Vinković, PhD for useful comments and discussion. This work was supported by the Croatian Science Foundation (IP-2013-11-4307). Authors acknowledge University of Zagreb, University Computing Centre (SRCE) for granting computational time on ISABELLA cluster.

References

1 S. C. Bergmeier, *Tetrahedron*, 2000, **56**, 2561–2576.
2 O. K. Karjalainen and A. M. P. Koskinen, *Org. Biomol. Chem.*, 2012, **10**, 4311.
3 U. V. S. Reddy, M. Chennapuram, C. Seki, E. Kwon, Y. Okuyama and H. Nakano, *Eur. J. Org. Chem.*, 2016, 4124–4143.
4 *Foye's principles of medicinal chemistry*, ed. W. O. Foye, T. L. Lemke and D. A. Williams, Wolters Kluwer Health/Lippincott Williams & Wilkins, Philadelphia, 7th edn, 2013.
5 M. G. Matera, C. P. Page, L. Calzetta, P. Rogliani and M. Cazzola, *Pharmacol. Rev.*, 2020, **72**, 218–252.
6 P. Gupta and N. Mahajan, *New J. Chem.*, 2018, **42**, 12296–12327.
7 C. Schneider, *Synthesis*, 2006, 3919–3944.
8 R.-E. Parker and N. S. Isaacs, *Chem. Rev.*, 1959, **59**, 737–799.
9 J. Liu, D. Zhou, X. Jia, L. Huang, X. Li and A. S. C. Chan, *Tetrahedron: Asymmetry*, 2008, **19**, 1824–1828.
10 F. Baur, D. Beattie, D. Beer, D. Bentley, M. Bradley, I. Bruce, S. J. Charlton, B. Cuenoud, R. Ernst, R. A. Fairhurst, B. Faller, D. Farr, T. Keller, J. R. Fozard, J. Fullerton, S. Garman, J. Hatto, C. Hayden, H. He, C. Howes, D. Janus, Z. Jiang, C. Lewis, F. Loeuillet-Ritzler, H. Moser, J. Reilly, A. Steward, D. Sykes, L. Tedaldi, A. Trifilieff, M. Tweed, S. Watson, E. Wissler and D. Wyss, *J. Med. Chem.*, 2010, **53**, 3675–3684.
11 A. Bosak, I. Gazić Smilović, G. Šinko, V. Vinković and Z. Kovarik, *J. Med. Chem.*, 2012, **55**, 6716–6723.
12 N. Arnold, D. Beattie, M. Bradley, A. Brearley, L. Brown, S. J. Charlton, R. A. Fairhurst, D. Farr, J. Fozard, J. Fullerton, M. Gosling, J. Hatto, D. Janus, D. Jones, L. Jordan, C. Lewis, J. Maas, C. McCarthy, M. Mercer, H. Oakman, N. Press, R. Profit, F. Schuerch, D. Sykes, R. J. Taylor, A. Trifilieff and A. Tuffnell, *Bioorg. Med. Chem. Lett.*, 2014, **24**, 4341–4347.
13 G. Xing, L. Pan, C. Yi, X. Li, X. Ge, Y. Zhao, Y. Liu, J. Li, A. Woo, B. Lin, Y. Zhang and M. Cheng, *Bioorg. Med. Chem.*, 2019, **27**, 2306–2314.
14 M. Stanek, L.-P. Picard, M. F. Schmidt, J. M. Kaindl, H. Hübner, M. Bouvier, D. Weikert and P. Gmeiner, *J. Med. Chem.*, 2019, **62**, 5111–5131.
15 C. Yi, G. Xing, S. Wang, X. Li, Y. Liu, J. Li, B. Lin, A. Y.-H. Woo, Y. Zhang, L. Pan and M. Cheng, *Bioorg. Med. Chem.*, 2020, **28**, 115178.
16 P. A. Glossop, C. A. L. Lane, D. A. Price, M. E. Bunnage, R. A. Lewthwaite, K. James, A. D. Brown, M. Yeadon, C. Perros-Huguet, M. A. Trevethick, N. P. Clarke, R. Webster, R. M. Jones, J. L. Burrows, N. Feeder, S. C. J. Taylor and F. J. Spence, *J. Med. Chem.*, 2010, **53**, 6640–6652.
17 A. Liu, L. Huang, Z. Wang, Z. Luo, F. Mao, W. Shan, J. Xie, K. Lai and X. Li, *Bioorg. Med. Chem. Lett.*, 2013, **23**, 1548–1552.
18 R. M. McKinnell, U. Klein, M. S. Linsell, E. J. Moran, M. B. Nodwell, J. W. Pfeiffer, G. R. Thomas, C. Yu and J. R. Jacobsen, *Bioorg. Med. Chem. Lett.*, 2014, **24**, 2871–2876.
19 L. H. Jones, J. Burrows, N. Feeder, P. Glossop, K. James, R. M. Jones, A. S. Kenyon, S. Patel, D. F. Roberts, M. D. Selby, R. S. Strang, E. F. Stuart, M. A. Trevethick, J. Watson, K. N. Wright and N. Clarke, *Bioorg. Med. Chem. Lett.*, 2015, **25**, 5121–5126.
20 J. C. Barrow, P. G. Nantermet, H. G. Selnick, K. L. Glass, P. L. Ngo, M. B. Young, J. M. Pellicore, M. J. Breslin, J. H. Hutchinson, R. M. Freidinger, C. Condra, J. Karczewski, R. A. Bednar, S. L. Gaul, A. Stern, R. Gould and T. M. Connolly, *Bioorg. Med. Chem. Lett.*, 2001, **11**, 2691–2696.
21 C. Lu, Z. Luo, L. Huang and X. Li, *Tetrahedron: Asymmetry*, 2011, **22**, 722–727.
22 Q. Ye, T. Cheng, Y. Zhao, J. Zhao, R. Jin and G. Liu, *ChemCatChem*, 2015, **7**, 1801–1805.
23 J. Wu, Y. Tian, S. Wang, M. Pistolozzi, Y. Jin, T. Zhou, G. Roy, L. Xu and W. Tan, *Eur. J. Med. Chem.*, 2017, **126**, 61–71.
24 A. González-Antuña, I. Lavandera, P. Rodríguez-González, J. Rodríguez, J. I. García Alonso and V. Gotor, *Tetrahedron*, 2011, **67**, 5577–5581.
25 M. Nery, M. Azevedo, J. Cardoso, G. Slana, R. Lopes and C. Lopes, *Synthesis*, 2007, 1471–1474.
26 M. Nery, M. Azevedo, J. Cardoso, G. Slana, R. Lopes and C. Lopes, *Synthesis*, 2016, 462–462.
27 L.-L. Gan, M.-W. Wang, M.-S. Cheng and L. Pan, *Biol. Pharm. Bull.*, 2003, **26**, 323–328.
28 X. Ge, A. Y.-H. Woo, G. Xing, Y. Lu, Y. Mo, Y. Zhao, Y. Lan, J. Li, H. Yan, L. Pan, Y. Zhang, B. Lin and M. Cheng, *Eur. J. Med. Chem.*, 2018, **152**, 424–435.
29 X. Ge, Y. Mo, G. Xing, L. Ji, H. Zhao, J. Chen, B. He, X. Chen, R. Xing, X. Li, Y. Zhao, J. Li, H. Yan, A. Y.-H. Woo, Y. Zhang, B. Lin, L. Pan and M. Cheng, *Bioorg. Chem.*, 2018, **79**, 155–162.

30 A. Bosak, A. Knežević, I. Gazić Smilović, G. Šinko and Z. Kovarik, *J. Enzyme Inhib. Med. Chem.*, 2017, **32**, 789–797.
31 D. I. Ball, R. T. Brittain, R. A. Coleman, L. H. Denyer, D. Jack, M. Johnson, L. H. C. Lunts, A. T. Nials, K. E. Sheldrick and I. F. Skidmore, *Br. J. Pharmacol.*, 1991, **104**, 665–671.
32 J. M. Grisar, G. P. Claxton, T. M. Bare, R. C. Dage, H. C. Cheng and J. K. Woodward, *J. Med. Chem.*, 1981, **24**, 327–336.
33 D. T. Collin, D. Hartley, D. Jack, L. H. Lunts, J. C. Press, A. C. Ritchie and P. Toon, *J. Med. Chem.*, 1970, **13**, 674–680.
34 Y. Rong and A. E. Ruoho, *Synth. Commun.*, 1999, **29**, 2155–2162.
35 Z.-L. Guo, Y.-Q. Deng, S. Zhong and G. Lu, *Tetrahedron: Asymmetry*, 2011, **22**, 1395–1399.
36 R. Hett, R. Stare and P. Helquist, *Tetrahedron Lett.*, 1994, **35**, 9375–9378.
37 M. M. Toteva and J. P. Richard, in *Advances in Physical Organic Chemistry*, Elsevier, 2011, vol. 45, pp. 39–91.
38 W. Li, X. Xu, P. Zhang and P. Li, *Chem. – Asian J.*, 2018, **13**, 2350–2359.
39 D. Richter, N. Hampel, T. Singer, A. R. Ofial and H. Mayr, *Eur. J. Org. Chem.*, 2009, 3203–3211.
40 M. Kazim, M. A. Siegler and T. Lectka, *Org. Lett.*, 2019, **21**, 2326–2329.
41 Y. You, B.-X. Quan, Z.-H. Wang, J.-Q. Zhao and W.-C. Yuan, *Org. Biomol. Chem.*, 2020, **18**, 4560–4565.
42 M. F. McLaughlin, E. Massolo, T. A. Cope and J. S. Johnson, *Org. Lett.*, 2019, **21**, 6504–6507.
43 V. Simeon-Rudolf and B. Juršić, *Period. Biol.*, 1996, **98**, 331–335.
44 P. Masson, M.-T. Froment, C. F. Bartels and O. Lockridge, *Eur. J. Biochem.*, 1996, **235**, 36–48.
45 D. Middlemiss and K. J. Ingold, US20110230555A1, 2011.
46 A. D. Becke, *J. Chem. Phys.*, 1993, **98**, 5648–5652.
47 T. H. Dunning, *J. Chem. Phys.*, 1989, **90**, 1007–1023.
48 A. V. Marenich, C. J. Cramer and D. G. Truhlar, *J. Phys. Chem. B*, 2009, **113**, 6378–6396.
49 S. Grimme, *J. Chem. Phys.*, 2006, **124**, 034108.
50 S. Grimme, S. Ehrlich and L. Goerigk, *J. Comput. Chem.*, 2011, **32**, 1456–1465.
51 L. Goerigk and S. Grimme, *J. Chem. Theory Comput.*, 2011, **7**, 291–309.
52 M. J. Frisch, G. W. Trucks, H. B. Schlegel, G. E. Scuseria, M. A. Robb, J. R. Cheeseman, G. Scalmani, V. Barone, G. A. Petersson, H. Nakatsuji, X. Li, M. Caricato, A. V. Marenich, J. Bloino, B. G. Janesko, R. Gomperts, B. Mennucci, H. P. Hratchian, J. V. Ortiz, A. F. Izmaylov, J. L. Sonnenberg, D. Williams-Young, F. Ding, F. Lipparini, F. Egidi, J. Goings, B. Peng, A. Petrone, T. Henderson, D. Ranasinghe, V. G. Zakrzewski, J. Gao, N. Rega, G. Zheng, W. Liang, M. Hada, M. Ehara, K. Toyota, R. Fukuda, J. Hasegawa, M. Ishida, T. Nakajima, Y. Honda, O. Kitao, H. Nakai, T. Vreven, K. Throssell, J. A. Montgomery Jr., J. E. Peralta, F. Ogliaro, M. J. Bearpark, J. J. Heyd, E. N. Brothers, K. N. Kudin, V. N. Staroverov, T. A. Keith, R. Kobayashi, J. Normand, K. Raghavachari, A. P. Rendell, J. C. Burant, S. S. Iyengar, J. Tomasi, M. Cossi, J. M. Millam, M. Klene, C. Adamo, R. Cammi, J. W. Ochterski, R. L. Martin, K. Morokuma, O. Farkas, J. B. Foresman and D. J. Fox, *Gaussian 16*, Gaussian, Inc., Wallingford CT, 2016.
53 R. T. Evans and M. J. McQueen, *CRC Crit. Rev. Clin. Lab. Sci.*, 1986, **23**, 35–64.
54 G. L. Ellman, K. D. Courtney, V. Andres and R. M. Featherstone, *Biochem. Pharmacol.*, 1961, **7**, 88–95.
55 V. Simeon-Rudolf, G. Šinko, A. Štuglin and E. Reiner, *Croat. Chem. Acta*, 2001, **74**, 173–182.
56 W. N. Aldridge and E. Reiner, *Enzyme inhibitors as substrates: interactions of esterases with esters of organophosphorus and carbamic acids*, North-Holland, New York, 1972, vol. 26.